Proceedings World Geothermal Congress 2010
Bali, Indonesia, 25-29 April 2010

Numerical Simulation of Variable-Density Flow in a Rock Represented by Multidimensional Model

Milan Hokr, Jiri Maryska, Otto Severyn, and Jirina Kralovcova

NTI, Technical University of Liberec, Studentska 2, Liberec, 46117, Czech Republic

Milan.hokr@email.cz

Keywords: finite element methods, fracture flow, groundwater, coupled processes

ABSTRACT

Prediction of coupled phenomena of heat and solute transport and water flow is important tool for dimensioning geothermal applications. We present a model and numerical simulation software, where the variable-density coupling effect is implemented to the combination of equivalent continuum and discrete fracture network (so called multidimensional model). We compare several algorithms for dealing with the non-linear terms. The importance of large-scale fractures to the qualitative and quantitative evaluation is demonstrated on model problems.

1. INTRODUCTION

Modeling of the groundwater flow and solute transport is important in many underground engineering activities and especially in planning and dimensioning a use of geothermal energy. The main problems from both the view of hydrogeology and computation are connected with complex geometrical description of fractured rock heterogeneity and many couplings between flow, transport, and chemical processes.

In this paper we study the combination of the variable-density flow problem (as an example of coupled non-linear problem) and a multidimensional representation of the fractured rock environment (as an example of geometric complexity). The variable-density flow is well known challenge for numerical computation from the last decades (Diersch and Kolditz, 2002), but yet studied mostly in the context of homogenized porous media (or fractured rock represented as continuum). The multidimensional approach consists of combining continuum and discrete fracture network representation of the rock environment to compromise the accuracy of representation, input data availability, and computational demands (Severyn et al 2006)

There are in general two major influences to the water (or solution) density in the context of flow phenomena: a decrease of density by thermal expansion and an increase of density by dissolved mass. There is an analogue in the flow field (mirrored vertically with respect to either an increase or a decrease of density) but a qualitatively different model of solute or heat transport: for heat distribution both rock conduction and water transport are significant, while the solute is only transported by water.

In this paper we aim on demonstration of “competition” between hydraulic gradient and density-gravity driving forces, with buoyancy pathways determined by the fracture network, to express the presented model concept effects. Thus we chose the case of solute driven variable-density problem, for which the simulation code was simpler to adapt. An example on how the heat conduction solution can be added, but without the variable-density effect, is presented in Cisarova et al (2010) on a case of real-world geological condition.

2. MODEL GOVERNING EQUATIONS

We assume the fluid flow is governed by the Darcy-type law, i.e. potential flow in each 1D, 2D, and 3D domain. The interaction between domains is consistently given by corresponding linear flux-pressure relation (transmissivity coefficient σ). The transport problem is governed by the advection-diffusion equation (in each subdomain), the exchange between the 1D, 2D and 3D domains is included in the advective fluxes.

We denote the problem domain $\Omega = \Omega_1 \cup \Omega_2 \cup \Omega_3$, $\Omega_i \subset R_3$, $i = 1,2,3$, where Ω_3 is a polyhedron (3D continuum), Ω_2 is a system of planar polygons (discrete fracture network) and Ω_1 is a system of lines (intersections of fractures = ``pipes").

The governing equations of flow are (for $i = 1,2,3$ the subdomain dimensions):

$$\vec{u}_i = K_i(\nabla p_i + \frac{\rho(c_i) - \rho_0}{\rho_0}\nabla z) \quad \text{in } \Omega_i \tag{1}$$

$$\kappa_i \frac{\partial p_i}{\partial t} - \nabla \cdot \vec{u}_i = q_i^+ + q_i^- + \sum_{j=1, j\neq i}^{3} \frac{\tilde{q}_{ij}}{\mu_i} \quad \text{in } \Omega_i \tag{2}$$

$$\tilde{q}_{ij} = \sigma_{ij}(p_i - p_j) \qquad i \neq j \tag{3}$$

where the unknowns are $u_i(\vec{x},t)$ the velocity and $p_i(\vec{x},t)$ the piezometric head, the parameters are K_i the hydraulic conductivity, κ_i the storativity, q_i sources/sinks, σ_{ij} transmissivity between domains, $\rho(c)$ density dependent on concentration, ρ_0 freshwater density. The auxiliary variable $\tilde{q}_{ij}$ denotes the flux between domains of different dimensionality (positive from j to i). The additional dimension μ_i ensures the compatible physical dimension of all flux variables: μ_1 is cross-sectional area of 1D domain, μ_2 is thickness of 2D domain, and $\mu_3 = 1$ (but the thickness is not considered when defining the positions and intersections of fractures).

The boundary conditions are prescribed on two different parts of the boundary $\partial\Omega_i = \Gamma_{i,D} \cup \Gamma_{i,N}$, $\Gamma_{i,D} \neq \emptyset$, $\Gamma_{i,D} \cap \Gamma_{i,N} = \emptyset$,

$$p_i = p_{i,D} \quad \text{on } \Gamma_{i,D} \tag{4}$$

$$\vec{u}_i \cdot \vec{v}_i = u_{i,N} \quad \text{on } \Gamma_{i,N} \tag{5}$$

where $p_{i,D}$ is the prescribed piezometric head (Dirichlet boundary condition) and $u_{i,N}$ is the prescribed flux (Neumann boundary condition).

The governing equations of the solute transport are for $i = 1,2,3$:

$$n_i \frac{\partial c_i}{\partial t} = -\nabla \cdot (c_i \vec{u}_i) + \nabla \cdot (\mathbf{D}_h^{(i)} \nabla c_i) + q_i^+ c_i^* + q_i^- c_i + \sum_{j=1, j\neq i}^{3} \frac{\tilde{q}_{ij}^{(c)}}{\mu_i}, \tag{6}$$

$$[\mathbf{D}_h]_{kl} = \delta_{kl} D_m + \alpha_T . |\mathbf{u}| . \delta_{kl} + (\alpha_L - \alpha_T) \frac{u_k u_l}{|\mathbf{u}|}, \tag{7}$$

where the unknowns are c_i solute concentrations, the parameters are $\mathbf{D}_h$ tensor of hydrodynamic dispersion, c_i^* injected concentration, $\tilde{q}_{ij}^{(c)}$ auxiliary solute source/sink due to interaction between domains,

$$\tilde{q}_{ij}^{(c)} = \begin{cases} \tilde{q}_{ij} c_j & \text{for } \tilde{q}_{ij} > 0 \\ \tilde{q}_{ij} c_i & \text{for } \tilde{q}_{ij} < 0. \end{cases} \tag{8}$$

The coupling between the flow and transport problems is by the velocity $\vec{u}_i$ and concentration-dependent density which is in general a nonlinear function obtained by measurement, but is considered as a linear approximation $\rho(c) = \rho_0 + \alpha c$ in our model. In the case of a multicomponent/multispecies solute transport, it can be simply extended to a linear combination of all the components, each with its own coefficient α.

3. NUMERICAL SIMULATION SOFTWARE

For the fluid flow (equations (1) and (2)) solution we use the mixed-hybrid finite element method, with the lowest order Raviart-Thomas space on tetrahedral, triangles, and line segments. The result unknowns are fluxes between the elements, which are the input for the scheme of transport equations solution. The particular adjustment for the multidimensional domain is presented in Kralovcova et al. (2006).

The transport problem (6) is solved by the finite volume method, with cell-centered concentration values, upwind weighting for the advective term, and explicit time stepping.

3.1 Algorithms for Variable-Density Coupling

We use two different options for dealing with flow-transport coupling through the variable density, distinguished by accuracy of the approximation. For expressing the algorithms, we use the following notation for the discrete unknowns (respective values of unknowns associated with nodes and elements): **P** is the vector of piezometric head values, **U** is the vector of flux values (velocity approximation), **C** is the vector of concentration values, and *n* denotes the time step counter.

The semi-coupled (explicit) scheme is the simpler one, where in each time step the flow field is calculated from the current distribution of density and from its results, the step of solute transport is calculated (Figure 1). The advantage is the computing speed (no significant rise compared to constant-density case), but problems can be with stability and accuracy for larger time step of switching between flow and transport calculation.

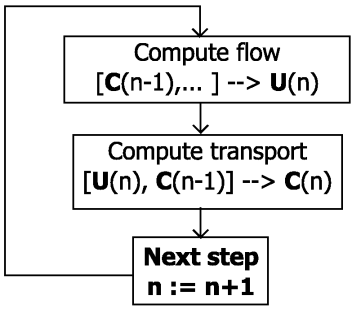

Figure 1: Scheme of the semi-coupled (explicit) solution algorithm, using the data of the second process from previous solution step.

The fully-coupled (iterative, implicit) scheme repeats the flow and transport calculation in one physical time step, until a convergence is reached, i.e. when we obtain new state of concentration from the previous one in the flow field corresponding to density from the new values of concentration (Figure 2). This method requires several times more computational time (due to repeated iterations) and the convergence is not guaranteed, but once reached, the modeled values will not "run away" from the physically realistic state.

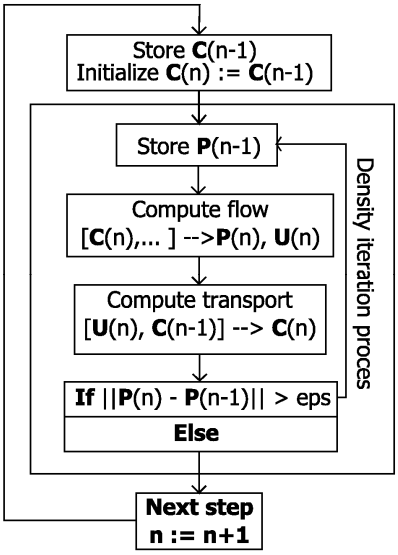

Figure 2: Scheme of the fully-coupled (implicit) solution algorithm, iterating to fit the data used for the given solution equal to the results of the respective step.

3.2 Numerical Simulation Code FLOW123D

The presented algorithms for coupling the flow and transport through the variable-density phenomenon has been implemented in the FLOW123D simulation code. The code is developed at the Technical university of Liberec and includes the model concepts and numerical methods in the paper by Severyn et al (2006) cited in the beginning.

The new options in the control file correspond to variable-density problems and presented numerical approaches:

switching the variable-density on/off, choice of weakly coupled (explicit) or fully coupled (iterative) scheme, time step size between the flow field recalculation iterations, input of weighting coefficients in the linear approximation of density in concentrations (for the respective species in the solution), choice of variably detailed output (flow and concentration field during the iterations), maximum iterations when no convergence is reported.

4. MODEL PROBLEMS

We demonstrate the simulated phenomena and properties of numerical solution on an example of vertical square domain 5×5 m with one-dimensional synthetic fracture network (Figure 3). The fracture network is discretized with 104 abscissa elements and the surrounding 2D continuum with 365 triangular elements. The flow boundary conditions are two prescribed piezometric heads $p = p_1$ and $p = p_2$ at the fractures (points) and no flow elsewhere. The transport boundary conditions are zero concentration in the given inflow/outflow points and zero flux elsewhere; the transport initial conditions are zero concentration in the domain except several elements with given $c_0 = 10\,\mathrm{kg/m^3}$, corresponding to the density ratio $\frac{\rho(c)-\rho_0}{\rho_0} = 0.01$ (with fresh water density 1000kg/m^3 and α=1). The positions are marked in Figure 3. The hydraulic conductivities are $K_1 = 5\,\mathrm{m/day}$ for 1D fractures and $K_2 = 0.1\,\mathrm{m/day}$ for 2D continuum (rock matrix).

The current version of the simulation code contains only the advective term. So the effect of dispersion is only represented by the numerical diffusion. In this case, the value of equivalent dispersities (either longitudinal or transversal) correspond to the discretisation size in the order of magnitude, i.e. 0.1-0.5m.

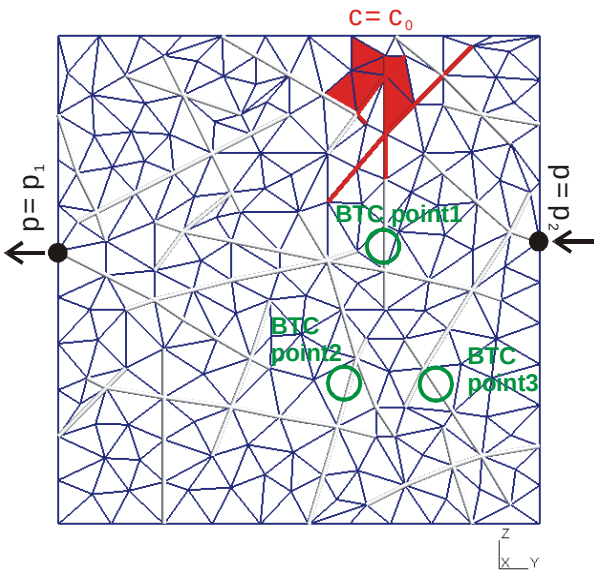

Figure 3: Fracture network (shaded gray), discretization of rock matrix (blue), position of piezometric head boundary condition (black), position of non-zero initial concentration position (red), and position of observation point for postprocessing (BTC=breakthrough curve) in green.

4.1 Comparison between Different Solution Algorithms

To check the sensitivity of results to choice of numerical algorithm and to evaluate the accuracy as dependent on discretisation, we compare the results between two algorithms presented in the section 3.1 and for various time step size keeping the total simulation time fixed.

The comparison is demonstrated by means of a graph of concentration changing in time in selected characteristic points (positions in Figure 3). The simulation is for the variable-density zero-gradient case. In Figure 4, the upper graph shows very good agreement between implicit and explicit algorithms, while in the lower graph (for twice larger time step), there are parts with visible differences. It confirms the expectation that both methods are theoretically equivalent in the limit of time step to zero while for larger time step the inaccuracies rise.

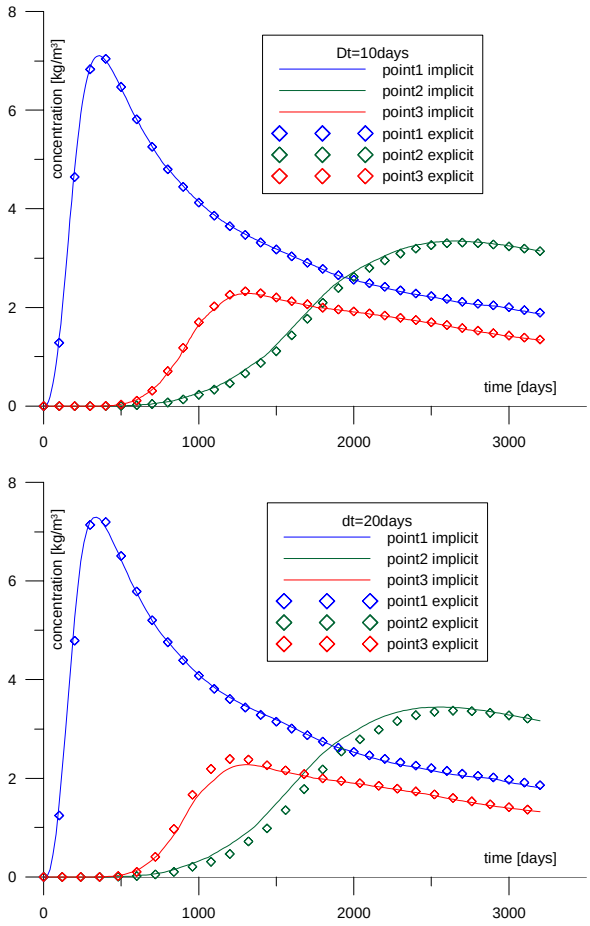

Figure 4: Comparison of implicit and explicit algorithm for variable-density coupling. The upper graph is for smaller time step dt=10 (better fit), the lower graph is for larger time step dt=20 (worse fit).

4.2 Comparison of Density Effect Versus Hydraulic Gradient

We consider three variants of flow boundary conditions with different hydraulic difference $p_2 - p_1$: 0, 0.001m, and 0.02m, leading to different qualitative behavior of the flow and transport processes. In the first one, the flow is governed only by the density variations. In the second case, the movement driven by density dominates, but the effect of hydraulic gradient is significant. In the third case, the hydraulic gradient dominates.

The expected effect of hydraulic gradient is the flow from the right input point to the left one, concentrated in the single connected fracture path with minor flow around, having quite small effect on transport outside of the fracture. The expected effect of variable density and gravity is downward flow in the place of higher concentration (density) and upward flow around, making the part with concentration "sinking".

The results, in the form of concentration and velocity distribution in the final time of simulation t=3200days, are displayed in Figure 5 in a comparative structure. The "rows" correspond to the respective three cases of hydraulic gradient. The left column is the constant-density (common flow and transport model) case and the right column is the variable-density case. Since there is no interest in the case of constant-density zero- gradient case (nothing happens), we present (as the exception from the above mentioned structure) the variable-density case in the initial time in the top left picture.

In the zero-gradient and small gradient cases (and variable-density model), we observe formation of buoyancy flows, which are preferentially oriented to the conductive fractures where available. Comparing initial and final state, we can see the movement of the concentration plume. There is almost no movement in the constant density small gradient case. For the large gradient, the movement in the constant-density model is already observable. The difference between constant-density and variable-density is small, but visible.

5. CONCLUSION

In the presented model we combined two complex model concepts – multidimensional geometry and variable-density coupling between the flow and the transport problems. The use of mixed-hybrid finite elements for numerical solution brings more flexibility to combination of fracture and matrix elements as both have independent discrete quantities. On the model problem, we demonstrated qualitative behavior where the convective cells characteristics for the variable-density flow are dominantly governed by the geometry of conductive fractures. The correctness of the coupling schemes is confirmed by comparing them to each other and observing the convergence with time step refinement.

ACKNOWLEDGEMENT

This work has been supported by the Ministry of Education of the Czech Republic (MŠMT), project number 1M0554.

REFERENCES

Císařová, K, Kopal, J, Královcová, J. and Maryška, J: Simulation of geothermal processes, submitted to World Geothermal Congress (this proceedings), 2010.

Diersch, H.J.G, and Kolditz, O: Variable-density flow and transport in porous media: approaches and challenges, *Adv. in Water Res*. 25 (2002), 899–-944.

Královcová, J., Maryška, J., Severýn, O., Šembera, J.: Formulation of mixed-hybrid FE model of flow in fractured porous medium. In: *Proceedings* of ENUMATH 2005, Springer-Verlag, 2006, pp. 1184-1191.

Severýn, O, Hokr, M, Královcová, J, and Maryška, J.: Modeling of groundwater flow and contaminant transport in hard rock using multidimensional FEM/FVM, GeoProc2006 Advances on Coupled Thermo-Hydro-Mechanical-Chemical Processes in Geosystems and Engineering, HoHai University, Nanjing, China, 2006, pp. 356–363.

Shikaze, S.G., Sudicky, E.A., Schwartz, F.W.: Density-dependent solute transport in discretely-fractured geologic media: is prediction possible?, *J. of Contam. Hydrol*. 34(1998), 273–291

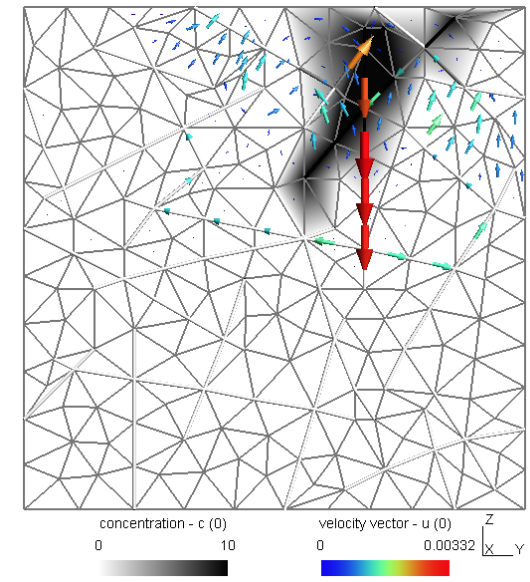

(a)

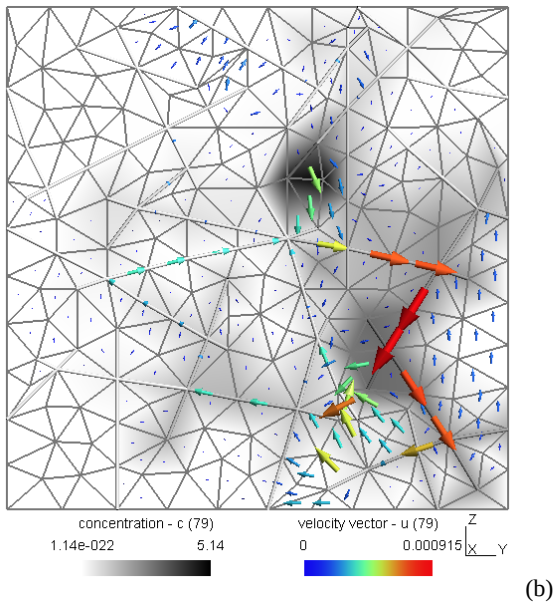

(b)

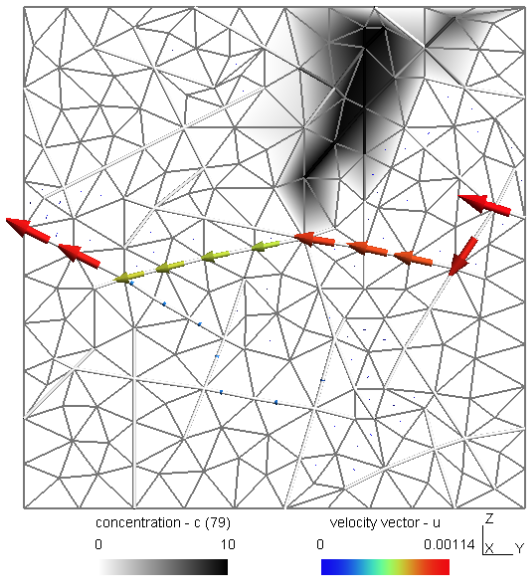

(c)

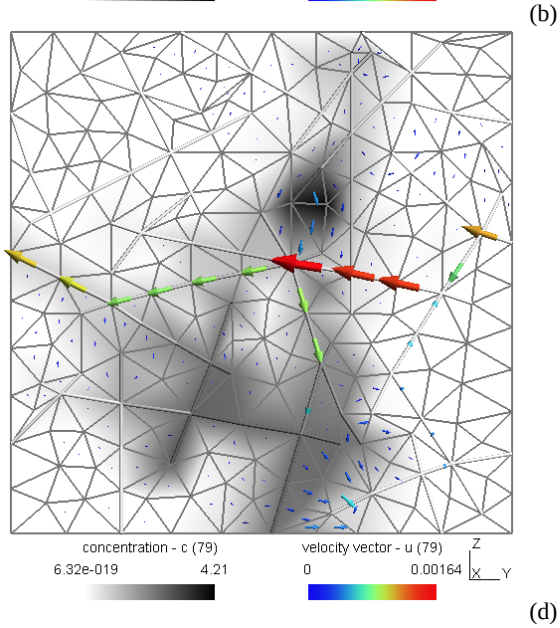

(d)

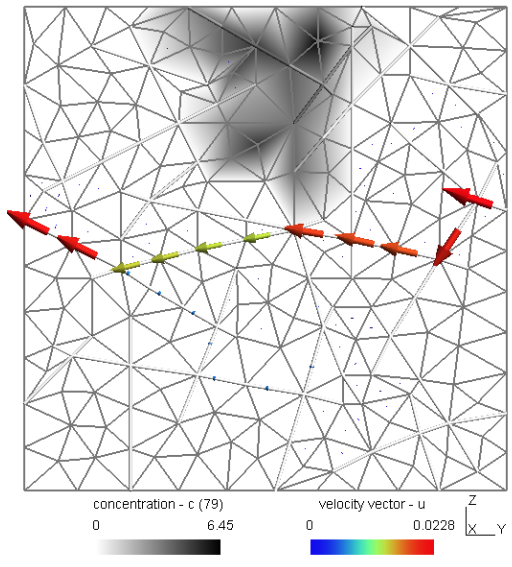

(e)

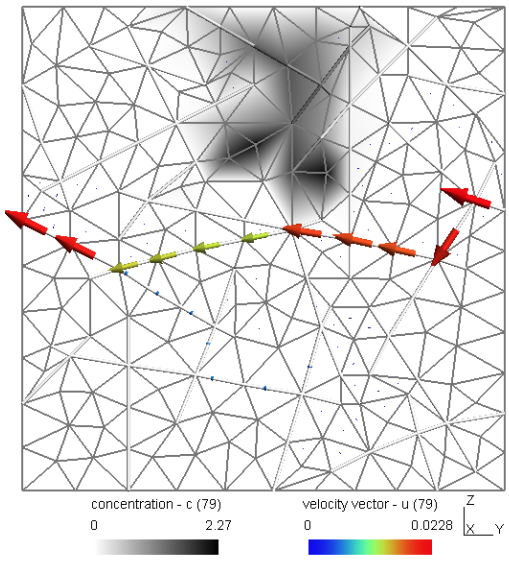

(f)

Figure 5: Results of the model problem: rows correspond to hydraulic gradient cases (a) zero difference, (c) (d) is 0.02m, and (e) (f) 0.001m difference.

Left "column" (c) and (e) is the constant-density model, the right "column (b) (d) (f) is the variable-density model. Figure (a) is the initial state.